



Predicting the Water Content of Interstellar Objects from Galactic Star Formation Histories

Chris Lintott¹ , Michele T. Bannister² , and J. Ted Mackereth^{3,4,5,6} ¹ Department of Physics, University of Oxford, Denys Wilkinson Building, Keble Road, Oxford, OX1 3RH, UK² School of Physical and Chemical Sciences—Te Kura Matū, University of Canterbury, Private Bag 4800, Christchurch 8140, New Zealand³ Canadian Institute for Theoretical Astrophysics, University of Toronto, 60 St. George Street, Toronto, ON, M5S 3H8, Canada⁴ Dunlap Institute for Astronomy and Astrophysics, University of Toronto, 50 St. George Street, Toronto, ON M5S 3H4, Canada⁵ David A. Dunlap Department for Astronomy and Astrophysics, University of Toronto, 50 St. George Street, Toronto, ON M5S 3H4, Canada

Received 2021 August 31; revised 2021 December 6; accepted 2021 December 9; published 2021 December 29

Abstract

Planetesimals inevitably bear the signatures of their natal environment, preserving in their composition a record of the metallicity of their system’s original gas and dust, albeit one altered by the formation processes. When planetesimals are dispersed from their system of origin, this record is carried with them. As each star is likely to contribute at least 10^{12} interstellar objects (ISOs), the Galaxy’s drifting population of ISOs provides an overview of the properties of its stellar population through time. Using the EAGLE cosmological simulations and models of protoplanetary formation, our modeling predicts an ISO population with a bimodal distribution in their water mass fraction: objects formed in low-metallicity, typically older, systems have a higher water fraction than their counterparts formed in high-metallicity protoplanetary disks, and these water-rich objects comprise the majority of the population. Both detected ISOs seem to belong to the lower water fraction population; these results suggest they come from recently formed systems. We show that the population of ISOs in galaxies with different star formation histories will have different proportions of objects with high and low water fractions. This work suggests that it is possible that the upcoming Vera C. Rubin Observatory Legacy Survey of Space and Time will detect a large enough population of ISOs to place useful constraints on models of protoplanetary disks, as well as galactic structure and evolution.

Unified Astronomy Thesaurus concepts: [Interstellar objects \(52\)](#); [Milky Way Galaxy \(1054\)](#); [Planetesimals \(1259\)](#)

1. Introduction

The discovery of 1I/‘Oumuamua (Meech et al. 2017) and 2I/Borisov,⁷ the first two interstellar objects (ISOs) detected while passing through our solar system, has stimulated interest in the properties of the population from which they are drawn. Such small bodies are likely to be produced by a wide variety of dynamical and physical processes, in common with the development of planetesimals (‘Oumuamua ISSI Team et al. 2019). There is strong evidence that the early history of planetary systems, including our own, includes a period where $\sim 90\%$ of a system’s planetesimals are ejected (Fernandez & Ip 1984; Izidoro et al. 2015; Raymond et al. 2020). Most of the remaining planetesimals are also expected to become unbound from their parent star in time, through stripping by the Galactic tide, stellar encounters, and in the post-main-sequence stages of stellar evolution (Kaib & Quinn 2009; Veras et al. 2011; Veras 2016; Pfalzner et al. 2021a).

In this work, we view these dispersed planetesimals as forming a population of ISOs with the potential to encounter our solar system. Each stellar system contributes to a progressively accumulated background population of ISOs that builds up through Galactic history (Moro-Martín et al.

2009; Moro-Martín 2018; Pfalzner & Bannister 2019), and which is then sampled as the solar system moves through the Milky Way. While more exotic processes may also contribute to the ISO population (see Levine et al. 2021 for an overview of current hypotheses), we address only planetesimal contributions in this initial study.

The properties of the ISOs that pass through our solar system are primarily determined by the material and conditions in the protoplanetary disks in which they formed. The dependence of the water abundance in protoplanetary bodies on the composition of their parent star has long been acknowledged, with the relative abundance of carbon and oxygen of particular importance (Delgado Mena et al. 2010; Johnson et al. 2012). More recent work by Cabral et al. (2019) developed a model of the expected composition of planetary building blocks on stellar metallicity; similar work by Santos et al. (2017) considered the dependence of water fraction of assembled, mature planets on initial metallicity. The model developed by Bitsch & Battistini (2020; hereafter BB20), discussed in detail below, also indicates that the properties of planetesimals are strongly dependent on disk metallicity. In particular, the BB20 model suggests that the water content of planetesimals that form beyond the ice line strongly depends on the availability or otherwise of oxygen.

Therefore, if we want to make predictions about observable quantities, such as the water content of ISOs such as ‘Oumuamua and 2I/Borisov, we need to consider the properties and metallicity of the protoplanetary disk population in the Milky Way. This paper is a first attempt to combine existing models for this purpose.

⁶ Banting Fellow.⁷ <https://minorplanetcenter.net/mpec/K19/K19RA6.html> and <https://minorplanetcenter.net/mpec/K19/K19S72.html>

Luckily, enormous progress has been made in recent years in producing models of the structural and chemical evolution of the galaxy (see, for example, reviews by Bland-Hawthorn & Gerhard 2016 and Helmi 2020). Galactic models are increasingly well constrained by data, particularly from Gaia (Gaia Collaboration et al. 2018) and ground-based spectral surveys such as GALAH (Buder et al. 2018) and APOGEE (Majewski et al. 2017). Detailed simulations that put galactic structure in a cosmological context have been developed, allowing the chemical evolution of components in Milky-Way-analog galaxies to be studied in detail (e.g., Crain et al. 2015; Schaye et al. 2015; Wetzel & Hopkins 2016; Nelson et al. 2019; Pillepich et al. 2019).

In this paper, we use the EAGLE suite of hydrodynamical cosmological simulations (Crain et al. 2015; Schaye et al. 2015) alongside the models of Bitsch & Battistini (2020) to explore the connection between galactic chemical evolution and the composition of the observed ISO population for the first time. This work demonstrates the interest and importance of this chemical evolutionary approach to predicting the properties of the ISO population, and conversely, to show how the properties of observed ISOs might constrain the Milky Way’s star formation history. Existing constraints on such models come primarily from observations of stellar abundance. Though these observations are clearly linked to the metallicity of the protoplanetary disk, thermal and chemical reprocessing will affect how the relative abundances of species within a protoplanetary disk differ from its natal molecular cloud (Fedele & Favre 2020). It is therefore possible that studies of large numbers of ISOs may eventually provide insight into such processes.

In this Letter, we briefly review our input models before deriving a prediction for the distribution of water content of the predicted ISO population. With a larger local population expected to be explored by the first few years of the Vera C. Rubin Observatory’s upcoming Legacy Survey of Space and Time (LSST; Ivezić et al. 2019), we hope that this paper is the beginning of an effort to place ISOs passing through our solar system in the context of Milky Way models.

2. Input Models

2.1. Planetesimal Formation and Composition

The detection of ‘Oumuamua requires that a large population of ISOs must exist. For instance, Meech et al. (2017) consider this together with the nondetections in a volume of thoroughly searched survey space over 17 yr to constrain the local density of similar ISOs as 10^{15} pc^{-3} . Do et al. (2018) similarly find a mass density of ISOs that is high enough to imply that every star is contributing to the population. The discovery of 2I/Borisov is consistent with a size distribution for these objects that implies that ISOs are common in our solar neighborhood (Jewitt et al. 2020). As discussed above, the origin of the bulk of this population will be planetesimal formation, and the properties of such objects must depend on conditions in the protoplanetary disk, and in particular, on the raw materials available. The connection between stellar metallicity and the presence and properties of planetary systems has been debated since the discovery of the first exoplanets, a connection between metallicity and the probability that the star hosts giant planets was first suspected when only a handful were known (Gonzalez 1997) and was quickly formalized. Fischer &

Valenti (2005) found that the formation probability for gas giant planets is related to the square of the metallicity. It may even be possible to predict which stars have planets based on their metallicity (Hinkel et al. 2019).

Recent work by Sousa et al. (2019) found, furthermore, that properties of planets, specifically their mass, may depend on stellar metallicity. Therefore, models of planet formation need to consider the composition of accreting material. While many models follow astronomical convention in using the stellar iron abundance ($[\text{Fe}/\text{H}]$) as a single metallicity parameter, scaling other atomic species as appropriate, we adopt the models of Bitsch & Battistini (2020) which consider abundances for several important elements separately: iron, silicon, magnesium, oxygen, and carbon.

In this paper, as described below, we will assume that the composition of the ISO population is determined by that of the parent population of protoplanetary objects. We will use the models of Bitsch & Battistini (2020), and refer the interested reader to the detailed description of their work. In brief, we should note that their model is derived from stellar abundances from the GALAH survey (Buder et al. 2018), which allows the relationship between overall metallicity parameterized by $[\text{Fe}/\text{H}]$ and the abundance of other elements to be measured. The authors then use a chemical model derived from Madhusudhan et al. (2017) and Bitsch et al. (2018) to predict the abundance of molecules and resulting composition of planetary building blocks formed on either side of the water ice line.⁸ For this initial work, we assume that the ISO population is exclusively drawn from planetesimals that are formed beyond the ice line. This assumption is consistent, for instance, with ISOs liberated from their systems of formation by intracluster stellar flybys (Pfalzner et al. 2021a), though it will not fully account for the effect of planetary migration and scattering; however, similar trends in composition are seen by BB20 either side of the ice line.

The outputs of the model are shown in Figure 10 in Bitsch & Battistini (2020). Though a variety of molecules show changes in mass fraction beyond the ice line, here we concentrate on the mass fraction in water, which shows the most significant decline in mass fraction as stellar metallicity increases.

While at low metallicities water accounts for roughly half the mass in the planetesimal population, as the metallicity increases, it becomes much less significant, with the formation of CO_2 , CH_4 , and CO through chemical pathways that compete with water formation favored instead. The mass fraction of water thus declines with metallicity.

For our study, we read predicted mass fractions for $[\text{Fe}/\text{H}]$ of -0.4 to 0.4 in intervals of 0.1 from Figure 10 in BB20, interpolating between the plotted values using a third-degree polynomial fitted to the data. We will need to extend the model to higher metallicity for the most recently formed stars. In these regimes we extrapolate beyond the limits of the BB20 models and treat the water mass fractions there as upper/lower limits. In practice we need only assume that the water mass fraction stays low beyond $[\text{Fe}/\text{H}] = 0.4$; this is justified as BB20 point out that increasing $[\text{C}/\text{O}]$ with $[\text{Fe}/\text{H}]$ in Milky Way stars indicates that water mass fractions should continue to decrease with metallicity and the expected trend continues well outside the BB20 $[\text{Fe}/\text{H}]$ range in data from the APOGEE DR16 results (Majewski et al. 2017; Ahumada et al. 2020).

⁸ The mode of planetesimal formation followed depends on whether the disk is locally cold enough to allow water ice to form.

2.2. Chemical Evolution Models

Understanding the distribution of chemical elements throughout galaxies is essential in trying to understand the formation history and subsequent evolution of such systems. Measurements of stellar metallicity from surveys such as APOGEE (Majewski et al. 2017) which include hundreds of thousands of stars provide a “fossil record” for our own galaxy. Such a record is necessarily affected by a strong selection function (APOGEE, for example, targets only red giants and obviously cannot observe massive stars that have already died), and so the data are interpreted with the help of cosmologically motivated, hydrodynamical simulations such as EAGLE (Crain et al. 2015; Schaye et al. 2015), which predict the star formation histories and evolution of many hundreds or thousands of systems, providing a historical record of their evolution which can be compared with APOGEE to identify Milky-Way-like systems. As such simulations contain details of every epoch of star formation rather than just those whose stars survive to the present day, they are invaluable in allowing us to derive from simulations a history of star formation for a galaxy like our own. In this paper, we will assume that ISOs are produced along with stars, inherit a composition appropriate to their metallicity (see previous section), and remain in the wandering population even when the stars that produced them have reached the end of their lives. We further assume that the population is mixed throughout the Milky Way, so that any star formed can contribute to the observed ISO population; more complex modeling of galactic dynamics is left for future work.

We begin by using a wide selection of galaxies from the Ref-L100N1504 simulated volume to explore how our predictions depend on the star formation history of the simulated galaxy, selecting all 2039 galaxies from the Ref-L100N1504 volume which have $10^{10} < M_* < 10^{11} M_\odot$.

We next follow Mackereth et al. (2018; hereafter M18), who investigate the chemical evolution of more than a hundred Milky-Way-like galaxies drawn from EAGLE (specifically, from the Ref-L100N1504 simulation). Galaxies included in the study were required to have stellar mass in the interval $M_* = (5-7) \times 10^{10} M_\odot$ and to be disk-dominated.⁹

Finally, we use data from a single simulated galaxy which, like the Milky Way, exhibits $[\alpha/\text{Fe}]$ bimodality (at fixed $[\text{Fe}/\text{H}]$) and a star formation history which allowed high- and low- $[\alpha/\text{Fe}]$ populations to evolve separately. This combination of properties is rare—only 6 of the 133 systems that meet the Milky-Way-like criteria used by M18 show similar features—and makes the system a good analog for our own galaxy. The complex history of gas accretion and star formation that takes place in the simulated galaxy and the determination of the properties described above, are discussed in detail by M18 in their Section 4.

Within the simulation, gas particles undergo star formation via a stochastic process, with a probability that depends on the star formation rate and the gas particle mass (see Schaye et al. 2015 and Crain et al. 2015 for details of the treatment of star formation and enrichment). When it occurs, star formation follows a pressure-dependent Kennicutt–Schmidt law and is assumed to produce a single stellar population with a Chabrier IMF (Chabrier 2003). We assume that a population of ISOs is

created at the moment of star formation, though, in practice, there will be a delay between the formation of the star and the creation of planetesimals and their expulsion from the system. As the majority of such expulsions will happen early in a star’s life (Pfalzner & Bannister 2019), we do not attempt to model this separately. We assume that the number of ISOs contributed to the background population is proportional to the mass of the star. This assumption is justified as the mass of observed protoplanetary disks scales in a roughly linear fashion with the mass of the star (Andrews et al. 2013). Large ISOs will be long-lived, and so once added to the galactic population, they will persist (Guilbert-Lepoutre et al. 2016).

3. Results

3.1. Example Systems

We begin by using the mass and $[\text{Fe}/\text{H}]$ data provided by the simulations for each star particle in two example galaxies and the models from BB20 described in Section 2.1 to predict the water abundance of the ISOs in each system. We choose to focus on water as an abundant molecule and because the models of BB20 also show a much greater variation in water abundance with metallicity than other molecules. The water fraction of any observed and suitably bright ISO may potentially be determined from their comae, meaning that our model could be tested as more ISOs are found. By comparing two galaxies, we hope to illustrate the sensitivity of the ISO population’s predicted water-rich fraction to the details of their star formation histories. A large range in the predicted value would indicate that any model that predicts the observable properties of the ISO population would need to take into account the specific star formation history of the Milky Way. It would also suggest that observations of a significant number of ISOs might provide an independent observational test of the Milky Way star formation history.

The two galaxies have $5 < M_* < 7 \times 10^{10} M_\odot$. They differ in that one has star formation concentrated at early times, whereas the other has a more recent peak in star formation rate. Their star formation histories are shown in Figure 1(a), and the fraction of the predicted ISO population with a particular mass fraction in water in Figure 1(b). The galaxy with early star formation has an ISO population dominated by water-rich ISOs formed in low-metallicity systems, whereas in the system where star formation peaks more recently we gain a low-water mass fraction population formed in higher-metallicity systems.

For convenience later in the paper, we will quantify the differences in population by considering the fraction of water-rich ($f_{\text{H}_2\text{O}} > 0.4$) to water-poor ISOs. In the galaxy with only early star formation, this water-rich fraction is 0.74, whereas it is lower, at 0.32, for the galaxy with recent star formation. The difference indicates that a galaxy’s ISO population’s properties—at least in the case of the water mass fraction—does indeed depend on its star formation history.

3.2. Trends in the Galaxy Population

To further illustrate the sensitivity of our results to Galactic history, we compare the predicted water-rich fraction of the observed ISO population in a wider sample of galaxies drawn from the EAGLE simulation. For each, we compute their ISO population and mean stellar metallicity, $[\text{Fe}/\text{H}]$, as in Section 3.1. We then compute the fraction of water-rich ISOs (

⁹ The latter selection was carried out by requiring the fraction of kinetic energy carried by particles participating in ordered rotation to be greater than 0.4.

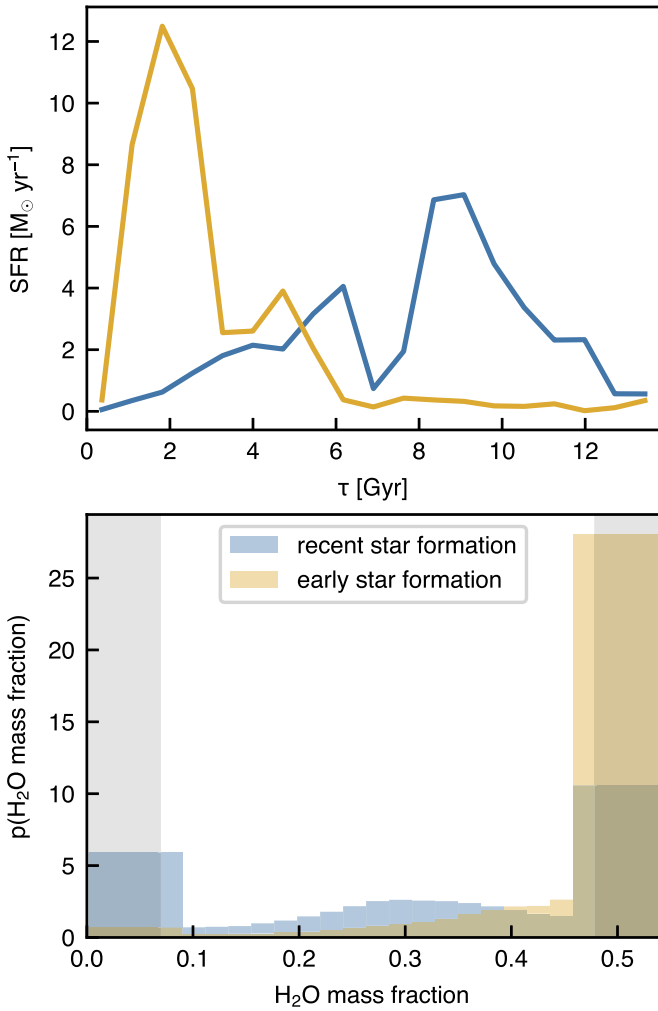


Figure 1. Top: star formation histories of two example galaxies (at fixed stellar mass) selected from EAGLE to demonstrate the ISO population predicted in a galaxy with recent star formation (blue) vs. one with earlier star formation (yellow). Bottom: predicted water mass fractions of ISO populations predicted for the galaxies shown above. The histograms are normalized such that $p(\text{H}_2\text{O mass fraction})$ is the probability density for finding an ISO in a given mass fraction bin or equivalently the fraction of the predicted ISO population in each bin.

i.e., those with an $f_{\text{H}_2\text{O}} > 0.4$) in each galaxy and compare this with the median age of its star particles.

In Figure 2, we show the median stellar age against the water-rich ISO fraction for these galaxies, coloring the points by the mean stellar metallicity of each galaxy. There is a significant trend such that older, more metal-poor galaxies have more water-rich ISO populations. At intermediate ages, the trend is less significant, but the correlation with $[\text{Fe}/\text{H}]$ demonstrates that strong constraints on the ISO population *and* Galactic mean metallicity would provide a good constraint on the Galactic star formation history. The fact that even as simple a proxy for the star formation history as the median age of star formation correlates well with an observable property of the ISO population demonstrates how the observed population of ISOs in the Milky Way could constrain its early star formation history. In particular, we note that a low water-rich fraction is incompatible with a star formation history where the median age is greater than approximately 10 Gyr. More complex modeling of—and comparisons between—the ISO population

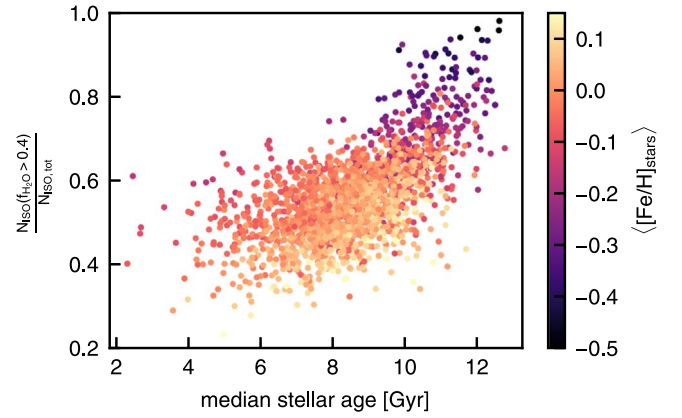


Figure 2. Water-rich ($f_{\text{H}_2\text{O}} > 0.4$) ISO fraction as a function of galaxy median age for 2039 galaxies with $10^{10} < M_* < 10^{11} M_{\odot}$ from the Ref-L100N1504 EAGLE volume. Points are colored by the mean stellar iron abundance relative to hydrogen, $[\text{Fe}/\text{H}]$, as a proxy for the overall metallicity; as expected, this quantity is linked to the star formation history. There is a clear trend between median stellar age and water-rich ISO fraction such that galaxies with older stellar populations harbor more water-rich ISOs.

and detailed Galactic star formation history will be the objective of future work.

3.3. Results for Milky Way Analog

We now consider predicting the ISO population for a single galaxy in the EAGLE simulation, the Milky Way analog described in Section 2.2. The results are shown in Figure 3. ISOs display a bimodal distribution, with 60% of the predicted population having $f_{\text{H}_2\text{O}} > 0.4$. A second substantial population is contributed by systems that form in higher-metallicity conditions, which, as noted earlier, have extremely low water fractions; 40% have $f_{\text{H}_2\text{O}} < 0.4$. The populations with $f_{\text{H}_2\text{O}} \gtrsim 0.4$ and $f_{\text{H}_2\text{O}} \lesssim 0.1$ come from stellar systems with $[\text{Fe}/\text{H}] \lesssim -0.3$ and $[\text{Fe}/\text{H}] \gtrsim 0.4$, respectively. The model therefore predicts that, as more ISOs are observed, the population should be dominated by twin populations of high and low water mass fractions, with relatively few ISOs appearing with an intermediate water fraction.

As expected from the enrichment history of the Milky Way, splitting the population by the age of the donor systems shows that this low water-fraction population comes from younger stars (formed within the last 4 Gyr), whereas ISOs with higher water fractions and low CO mass fractions are dominated by those formed around older stars. The presence of a population of ISOs with low water fraction is therefore an indication of a contribution from recent star formation. In general, if the observed ratio of high to low water-mass fraction ISOs varies from that predicted here, one must either adjust the adopted model of planetesimal formation, relax our assumption of rapid mixing, or change the details of the galactic evolutionary model. Recent work using data from Gaia (e.g., Mor et al. 2019) provide support for a model that suggests that the Milky Way has had a significant recent burst of star formation; our results suggest that observations of ISOs can provide a direct test of this idea.

3.4. Comparison with Observed ISOs

Having derived a broadly bimodal population, comprising both high and low water-fraction components, it is tempting to draw conclusions relative to the two ISOs observed so far.

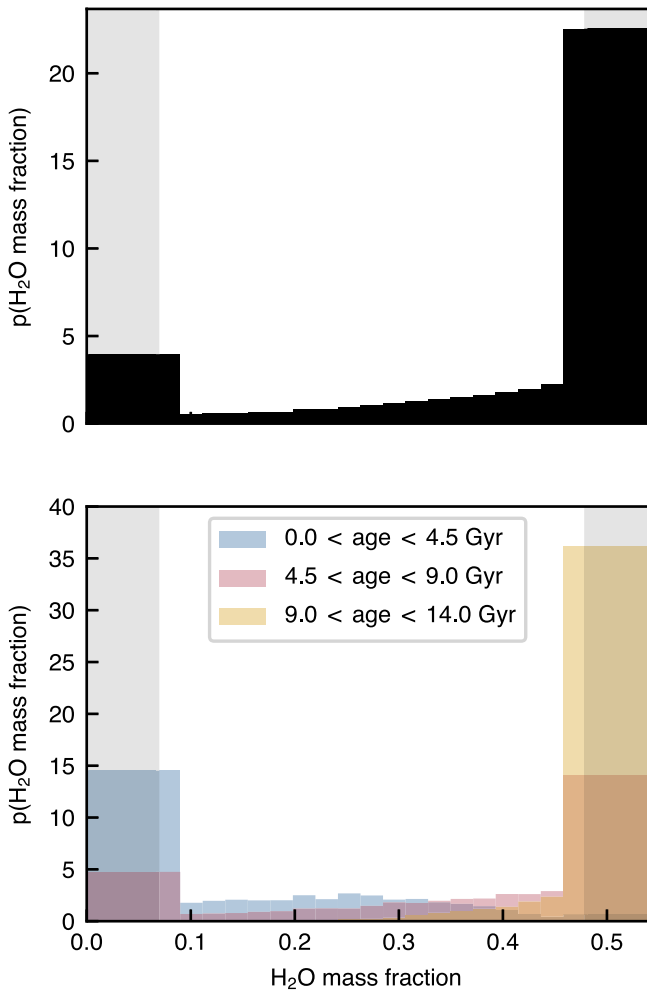


Figure 3. Top: predicted distribution of ISO objects by water-mass fraction. As before, the histograms are normalized such that $p(\text{H}_2\text{O mass fraction})$ is the probability density for finding an ISO in a given mass fraction bin or equivalently, the fraction of the predicted ISO population in each bin. The gray regions lie outside the formal limits of the BB20 model; here we assume that predicted ISOs have the minimum or maximum possible water mass fraction. Bottom: as above, but split by age of population. The low water-mass fraction population is dominated by the youngest objects, while the population with high water-mass fraction is from older systems.

Solar system experience advises caution in translating the dust-to-gas mass ratios inferred from one-off comae observations into refractory-to-ice mass ratios in the body (Choukroun et al. 2020). Considering ‘Oumuamua as a planetesimal, with a comet-colored surface but effectively inactive (Trilling et al. 2018; ‘Oumuamua ISSI Team et al. 2019), the tradeoffs in its dust-to-gas ratio versus its low bulk density leave its water fraction somewhat unconstrained (Hui & Knight 2019). 2I/Borisov’s coma showed water sublimation from at least 6 au, together with nitrogen and carbon (Fitzsimmons et al. 2018; Bannister et al. 2020). It is distinctively rich in CO relative to solar system comets (Bodewits et al. 2020; Cordiner et al. 2020). Seligman et al. (2021) argue that both of these ISOs can be plausibly considered CO-enriched planetesimals—if II had variable activity, a common state for comets.

In the context of the BB20 models, stars of supersolar metallicity have large carbon abundances, which binds into abundant CO and CO₂ exterior to the water line. Such disks would prolifically produce CO-rich objects. Consistently, the dynamical evidence suggests a young kinematic age for

‘Oumuamua—a mere 30–35 Myr, while 2I is dynamically hotter and thus older at around 700 Myr, though its age is not as well constrained (e.g., Hallatt & Wiegert 2020; Hsieh et al. 2021). Thus, both observed ISOs would be from the putative recently formed low water-fraction population. One from the high water-fraction population is yet to be seen. Speculatively, if ISOs with high water fractions form in low-metallicity disks, it may be that their dust-to-volatile ratio is different from that of their low water-fraction counterparts; lacking dust, such objects may quickly sublime in the outer solar system before they can be observed. Tempting though such speculation is, it is clear that drawing conclusions from two such briefly observed objects is obviously premature. It is certain that more observations, over longer timespans through perihelion, and best of all, one day from spacecraft ground-truth (see Comet Interceptor Snodgrass & Jones 2019), are needed to test these models.

Similarly, we suggest that information carried by the trajectories of observed ISOs also might be used to test the models. As an ISO travels through the Milky Way, it will be subject to on-average continuous dynamical heating, primarily from encounters with molecular clouds (Pfalzner et al. 2020) and dark matter substructure. Objects older than 1 Gyr will likely have been significantly heated vertically, and perhaps radially. An older population might thus be expected to have high velocity dispersion in all directions (McGlynn & Chapman 1989); this line of argument, if sustained by further modeling, would predict that the more water-rich ISOs will have a more isotropic distribution of origins on the sky than objects with lower water fractions. Adding a detailed understanding of Milky Way dynamics, derived from Gaia data, to our model will allow this prediction to be refined, in common with ISO trajectory expectations (Seligman & Laughlin 2018); this will lead to testable outcomes with the upcoming Vera C. Rubin Observatory sample.

Gaidos et al. (2017), and most recently, Hallatt & Wiegert (2020) and Hsieh et al. (2021) have suggested that the trajectory of ‘Oumuamua was consistent with membership in the nearby Carina local group. If the first ISO observed does indeed have a local origin, this would suggest that our assumption here of thorough mixing through the Galactic disk may need revision. There are also additional complexities of density such as stellar streams and individual stars’ ISO streams (e.g., Eubanks 2019; Portegies Zwart 2021).

However, this assignment of origin also seems to require unfeasible numbers of ISOs to be donated by each Carina stellar system, relative to the local solar ISO spatial density constraint. Pfalzner et al. (2021b) show that molecular clouds are regions of dense capture and release for ISOs. It is plausible that not all ISOs tracing to Carina originate in Carina stellar systems, and the molecular cloud is locally overdense with ISOs, perhaps as a consequence of cloud formation (see Pfalzner & Bannister 2019; Moro-Martín & Norman 2021).

4. Conclusions

This paper brings together two very different modeling efforts. The first, by Bitsch & Battistini (2020), predicts the composition of planetesimals formed beyond the ice line in a protoplanetary disk, and the second predicts the distribution of metallicity in Milky Way analogs from the EAGLE simulations (Crain et al. 2015; Schaye et al. 2015). We combine these efforts to predict the water mass fraction distribution for a

population of ISOs, assuming that the resulting population is well mixed and sampled randomly by the motion of our solar system through the galaxy.

The bulk of the resulting predicted ISO population has high ($[\text{Fe}/\text{H}] > 0.4$) water mass fractions, primarily from older systems that formed more than 4.5 Gyr ago. A second, smaller, but still substantial, population has low ($[\text{Fe}/\text{H}] < 0.1$) water mass fractions and is primarily due to more recent star formation; both ISOs seen thus far appear to belong to this population. As more ISOs are discovered, the relative frequency of those with high and low water fractions will provide a constraint on the effectiveness of mixing between old and young populations in the Milky Way, and this parameter also shows promise as a constraint on the Milky Way's star formation history. Such constraints from models could be compared with studies of stellar populations, providing tests of the same models with a different selection function. The ISO population will contain small bodies whose origins lie in systems where the central star has since died. Thus, studying such objects affords a different sampling of galactic star formation history than that possible from studies of extant stars.

This necessary preliminary study demonstrates the ability to make specific predictions about the nature of the ISO population from existing models. Extensions that consider the abundances of other molecules will add to the predictive power of our modeling. Further work that uses large-scale simulations such as EAGLE to provide insight into the nature of the ISO population is encouraged, and will be needed ahead of the beginning of the LSST to understand how properties of the observed population can be used to test the preliminary predictions presented here.

We thank the reviewer for their comments, which greatly helped in clarifying the arguments presented in this paper.

This paper benefited from much-appreciated discussions with Matthew Hopkins and the International Space Science Institute (ISSI) Oumuamua team in Bern, Switzerland, Susanne Pfalzner, Dennis Bodewits, Max Briel and Jan Eldridge, and Bruce Macintosh.

M.T.B. appreciates support by the Rutherford Discovery Fellowships from New Zealand Government funding, administered by the Royal Society Te Apārangi.

Software: Astropy (Astropy Collaboration et al. 2018), NumPy (Harris et al. 2020).

ORCID iDs

Chris Lintott  <https://orcid.org/0000-0001-5578-359X>

Michele T. Bannister  <https://orcid.org/0000-0003-3257-4490>

J. Ted Mackereth  <https://orcid.org/0000-0001-8108-0935>

References

- Ahumada, R., Prieto, C. A., Almeida, A., et al. 2020, *ApJS*, 249, 3
- Andrews, S. M., Rosenfeld, K. A., Kraus, A. L., & Wilner, D. J. 2013, *ApJ*, 771, 129
- Astropy Collaboration, Price-Whelan, A. M., & Sipőcz, B. M. 2018, *AJ*, 156, 123
- Bannister, M. T., Opatom, C., Fitzsimmons, A., et al. 2020, arXiv:2001.11605
- Bitsch, B., & Battistini, C. 2020, *A&A*, 633, A10
- Bitsch, B., Morbidelli, A., Johansen, A., et al. 2018, *A&A*, 612, A30
- Bland-Hawthorn, J., & Gerhard, O. 2016, *ARA&A*, 54, 529
- Bodewits, D., Noonan, J. W., Feldman, P. D., et al. 2020, *NatAs*, 4, 867
- Buder, S., Asplund, M., Duong, L., et al. 2018, *MNRAS*, 478, 4513
- Cabral, N., Lagarde, N., Reylé, C., Guilbert-Lepoutre, A., & Robin, A. C. 2019, *A&A*, 622, A49
- Chabrier, G. 2003, *PASP*, 115, 763
- Choukroun, M., Altwegg, K., Kühr, E., et al. 2020, *SSRv*, 216, 44
- Cordiner, M. A., Milam, S. N., Biver, N., et al. 2020, *NatAs*, 4, 861
- Crain, R. A., Schaye, J., Bower, R. G., et al. 2015, *MNRAS*, 450, 1937
- Delgado Mena, E., Israelian, G., González Hernández, J. I., et al. 2010, *ApJ*, 725, 2349
- Do, A., Tucker, M. A., & Tonry, J. 2018, *ApJL*, 855, L10
- Eubanks, T. M. 2019, *ApJL*, 874, L11
- Fedele, D., & Favre, C. 2020, *A&A*, 638, A110
- Fernandez, J. A., & Ip, W. H. 1984, *Icar*, 58, 109
- Fischer, D. A., & Valenti, J. 2005, *ApJ*, 622, 1102
- Fitzsimmons, A., Snodgrass, C., Rozitis, B., et al. 2018, *NatAs*, 2, 133
- Gaia Collaboration, Brown, A. G. A., Vallenari, A., et al. 2018, *A&A*, 616, A1
- Gaidos, E., Williams, J., & Kraus, A. 2017, *RNAAS*, 1, 13
- Gonzalez, G. 1997, *MNRAS*, 285, 403
- Guilbert-Lepoutre, A., Besse, S., Snodgrass, C., & Yang, B. 2016, in American Astronomical Society, DPS Meeting, 48 (Washington, DC: AAS), 116.12
- Hallatt, T., & Wiegert, P. 2020, *AJ*, 159, 147
- Harris, C. R., Millman, K. J., van der Walt, S. J., et al. 2020, *Natur*, 585, 357
- Helmi, A. 2020, *ARA&A*, 58, 205
- Hinkel, N. R., Unterborn, C., Kane, S. R., Somers, G., & Galvez, R. 2019, *ApJ*, 880, 49
- Hsieh, C.-H., Laughlin, G., & Arce, H. G. 2021, *ApJ*, 917, 20
- Hui, M.-T., & Knight, M. M. 2019, *AJ*, 158, 256
- Ivezić, Ž., Kahn, S. M., Tyson, J. A., et al. 2019, *ApJ*, 873, 111
- Izidoro, A., Morbidelli, A., Raymond, S. N., Hersant, F., & Pierens, A. 2015, *A&A*, 582, A99
- Jewitt, D., Hui, M.-T., Kim, Y., et al. 2020, *ApJL*, 888, L23
- Johnson, T. V., Mousis, O., Lunine, J. I., & Madhusudhan, N. 2012, *ApJ*, 757, 192
- Kaib, N. A., & Quinn, T. 2009, *Sci*, 325, 1234
- Levine, W. G., Cabot, S. H. C., Seligman, D., & Laughlin, G. 2021, *ApJ*, 922, 39
- Mackereth, J. T., Crain, R. A., Schiavon, R. P., et al. 2018, *MNRAS*, 477, 5072
- Madhusudhan, N., Bitsch, B., Johansen, A., & Eriksson, L. 2017, *MNRAS*, 469, 4102
- Majewski, S. R., Schiavon, R. P., Frinchaboy, P. M., et al. 2017, *AJ*, 154, 94
- McGlynn, T. A., & Chapman, R. D. 1989, *ApJL*, 346, L105
- Meech, K. J., Weryk, R., Micheli, M., et al. 2017, *Natur*, 552, 378
- Mor, R., Robin, A. C., Figueras, F., Roca-Fàbrega, S., & Luri, X. 2019, *A&A*, 624, L1
- Moro-Martín, A. 2018, *ApJ*, 866, 131
- Moro-Martín, A., & Norman, C. 2021, arXiv:2110.15366
- Moro-Martín, A., Turner, E. L., & Loeb, A. 2009, *ApJ*, 704, 733
- Nelson, D., Pillepich, A., Springel, V., et al. 2019, *MNRAS*, 490, 3234
- Oumuamua ISSI Team, Bannister, M. T., Bhandare, A., et al. 2019, *NatAs*, 3, 594
- Pfalzner, S., Aizpuru Vargas, L. L., Bhandare, A., & Veras, D. 2021a, *A&A*, 651, A38
- Pfalzner, S., & Bannister, M. T. 2019, *ApJL*, 874, L34
- Pfalzner, S., Davies, M. B., Kokaia, G., & Bannister, M. T. 2020, *ApJ*, 903, 114
- Pfalzner, S., Paterson, D., Bannister, M. T., & Portegies Zwart, S. 2021b, *ApJ*, 921, 168
- Pillepich, A., Nelson, D., Springel, V., et al. 2019, *MNRAS*, 490, 3196
- Portegies Zwart, S. 2021, *A&A*, 647, A136
- Raymond, S. N., Kaib, N. A., Armitage, P. J., & Fortney, J. J. 2020, *ApJL*, 904, L4
- Santos, N. C., Adibekyan, V., Dorn, C., et al. 2017, *A&A*, 608, A94
- Schaye, J., Crain, R. A., Bower, R. G., et al. 2015, *MNRAS*, 446, 521
- Seligman, D., & Laughlin, G. 2018, *AJ*, 155, 217
- Seligman, D., Levine, W. G., Cabot, S. H. C., Laughlin, G., & Meech, K. 2021, *ApJ*, 920, 28
- Snodgrass, C., & Jones, G. H. 2019, *NatCo*, 10, 5418
- Sousa, S. G., Adibekyan, V., Santos, N. C., et al. 2019, *MNRAS*, 485, 3981
- Trilling, D. E., Mommert, M., Hora, J. L., et al. 2018, *AJ*, 156, 261
- Veras, D. 2016, *RSOS*, 3, 150571
- Veras, D., Wyatt, M. C., Mustill, A. J., Bonsor, A., & Eldridge, J. J. 2011, *MNRAS*, 417, 2104
- Wetzel, A. R., Hopkins, P. F., Kim, J.-H., et al. 2016, *ApJL*, 827, L23